Springer

KSME

Journal of Mechanical Science and Technology 27 (7) (2013) 2191~2197
www.springerlink.com/content/1738-494x
DOI 10.1007/s12206-013-0535-7

Experimental and numerical analysis of natural convection heat transfer coefficient of V-type fin configurations †

Mohammad Mahdi Naserian*, Mahdi Fahiminia and Hamid Reza Goshayeshi

Department of Mechanical Engineering, Mashhad Branch, Islamic Azad University, Mashhad, Iran

(Manuscript Received November 15, 2011; Revised July 24, 2012; Accepted January 18, 2013)

Abstract

In the present study, the natural convection heat transfer coefficient from V-type fin-arrays on a vertical base is investigated both experimentally and numerically. The CFD simulations are carried out using Fluent software. The investigated cases consist of different shapes of a 90-degree V-type fin which are broken into discrete pieces instead of being an integrated fin. The number and shape of pieces as well as the gap between them is studied for different cases. By scrutinizing the results, an optimum fin shape on a vertical base is determined. In addition, the optimum V-type fin array is introduced by studying the number of rows for the optimum fin shape. Finally, a correlation is presented which relates the Nusselt number with the modified Rayleigh number.

Keywords: Experimental analysis; Heat transfer coefficient; Natural convection; V-type fin

1. Introduction

Due to the rapid development of technology, electronic devices are a part of our ordinary life. Considering multi-functioning, high clock speed, shrinking package size and higher power dissipation in electronic devices, the heat flux per unit area has increased dramatically over the past few years. Besides, the working temperature of the electronic components may exceed the desired temperature level. Thus, the effective removal of heat dissipations and maintaining the die at a safe operating temperature plays an important role to ensure a reliable operation of electronic components.

There are various methods to cool electronics, such as air flow cooling, heat pipe, etc. Air flow with heat sink was used in conventional electronics cooling systems which would show superiority in terms of unit price, weight and reliability. Therefore, the most common way to enhance the air-cooling is through the utilization of air flow on a heat sink.

In order to dispose the boundary layer restrictions and develop a compact high-performance heat transfer plate, some investigators have developed horizontal partition and V-shaped plates. Firstly, Misumi and Kitamura [1] have reported an experimental work on enhancement of natural convection heat transfer from vertical plate having a horizontal partition and V-shape plates in water circumference. They found that the heat transfer in the downstream region of the partition plate is remarkably enhanced when the plate height exceeds certain critical values due to the inflow of the low temperature fluid into the separation region. For vertical plate with V-shaped fins, the obtained heat transfer coefficient is 40% higher than the conventional fins. Furthermore, it is observed that the ratio of the heat transfer enhancement exceeds the ratio of the surface enlargement. Moreover, the enhancement obtained for horizontal partition plate and vertical fin is less than V-plate. This heat transfer enhancing technique is further investigated experimentally, in air as the circumference by Parishwad et al. [2].

Bhavnani and Bergles [3] used an interferometry technique to determine local heat transfer coefficients for surfaces with repeated ribs and steps. The ribbed surfaces, which were tested, had square cross-section with rib height of 6.35 and 3.18 mm, spaced at 25.4 mm intervals. The ribs were made of aluminum on vertical plate with constant wall temperature. The flow was laminar. The maximum increase in average heat transfer coefficient was 23.2% with a step pitch to-height ratio of 16. The study indicated the presence of an optimum step pitch-to-height ratio while all ribbed surfaces resulted in degraded heat transfer performance. The work by Heya et al. [4] suggests that the roughness elements which height is less than the boundary layer thickness will have no appreciable influence on the heat transfer of natural convection and these elements will work as flow retarder rather than the heat transfer promoter. The above mentioned references show the necessity of studying and optimization of V-type ribs on vertical base plate.

*Corresponding author. Tel.: +98 9158191285, Fax.: +98 5116215774
E-mail address: MmahNas@yahoo.com
† Recommended by Associate Editor Jun Sang Park

2. Experimental apparatus

The set-up consists of various instruments for measuring the ambient temperature, rear surface of the main heater temperature, the temperature of the front surface of guard heater the temperature of the air (as close as possible to fin configuration), close to fin configuration, and the input power of both heaters. Homogeneous and constant heating is ensured by using a thermo-foil laminar heater which is attached to the rear of the base plate in fin configuration. Special attention was paid for the insulation of the rear surface of the main heater. To choose a suitable insulation, we know that only the thickness (L) and the thermal conductivity (k) of insulation are important for the conduction of heat through it. Hence, the heat loss through plate can be eliminated by letting either L→∞ or k→0. Since a plate of L→∞ or k→0 is physically impossible, the foregoing insulation may never be accomplished in the absolute sense. However, the larger the thickness or the smaller the thermal conductivity, the better the insulation will be. If the heat loss through plate is desired to be completely eliminated, the use of another heater becomes necessary. The second heater, often referred to as the guard heater, is an important experimental tool for the control of heat transfer [5]. Then, by properly adjusting the power supply to the guard heater, all internal energy generated in the main heater may be transferred through other surfaces of it. Therefore, the gap between the rear surface of the main heater and the front surface of guard heater is filled by epoxy and hardener. The temperature of the surfaces of epoxy plate, which are in contact with heaters is adjusted at the same degree, which almost eliminates the heat loss from the rear surface of main heater. The lateral surfaces of both heaters and the rear surface of the guard heater are insulated by rock wool.

The experiments are conducted with constant temperature in air circumference excluding air currents. Fig. 1 shows the power circuit. The electrical power was supplied through a regulated AC power supply. The input power of the main heater could be selected precisely by feeding the power to a variable transformer (variac). The voltage drop and the current flow were monitored by a voltmeter-ammeter combination; the supplied power is calculated by multiplying the voltage drop and the current through the heater.

The temperatures beside the heat sink are presented by temperature patterns. For given Y_{exp} locations, we extract temperature profiles, expressed as temperature vs. the distance perpendicular to the heat sink of the measure T=f (Z_{exp}). Fig. 2 shows temperature profile beside the vertical plate. Equations for these curves are obtained by polynomial fitting. The calculated slope, which is deduced from curve equation, allows us to calculate local heat transfer coefficient, h_y. Therefore, the local Nusselt number is deduced from Eq. (1).

$$Nu_y = \frac{h_y Y_{exp}}{k} = \frac{\left.-k\dfrac{\partial T}{\partial Z_{exp}}\right)_{Z_{exp}=0} Y_{exp}}{k\left(T_s - T_\infty\right)} = \frac{\left.-\dfrac{\partial T}{\partial Z_{exp}}\right)_{Z_{exp}=0} Y_{exp}}{\left(T_s - T_\infty\right)} \tag{1}$$

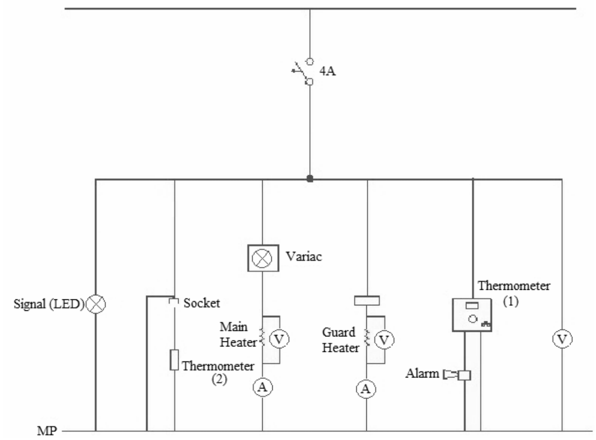

Fig. 1. Power circuit of experimental apparatus.

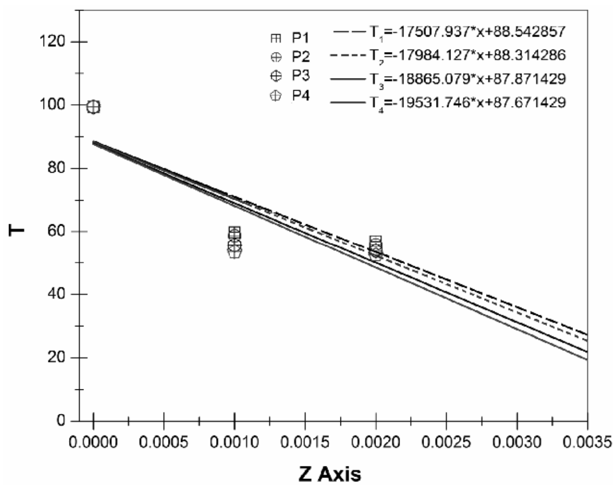

Fig. 2. Temperature profile beside the vertical plate (ΔT = 74.2).

where ΔZ_{exp} represents the space step in perpendicular direction to the plate, and T_i (i=1, 2, 3) is the successive temperature which is measured along a profile, beside the heat sink, along a profile $T = f(Z_{exp})$.

A schematic view of experimental setup and experimental apparatus is presented in Fig. 3. The material of heat sink is selected as aluminum alloy 6061 and has a thermal conductivity value of 168 W/m℃. The areas of the both heaters are 80 mm x 59.8 mm.

The accuracy of experimental results depends upon the accuracy of the individual measuring instruments and the manufacturing accuracy of the test section. Based on the error theory, the total uncertainty, U comprises of uncertainties of many experimental parameters, which influence on the experiment. For a value of M, whose results depend on uncorrelated input estimates $x_1, x_2, \ldots, x_N$, the standard measurement uncertainty is obtained by appropriately combining the standard uncertainties of these input estimates. The combined standard uncertainties of the estimate M denoted by U is calculated from the following equations [8].

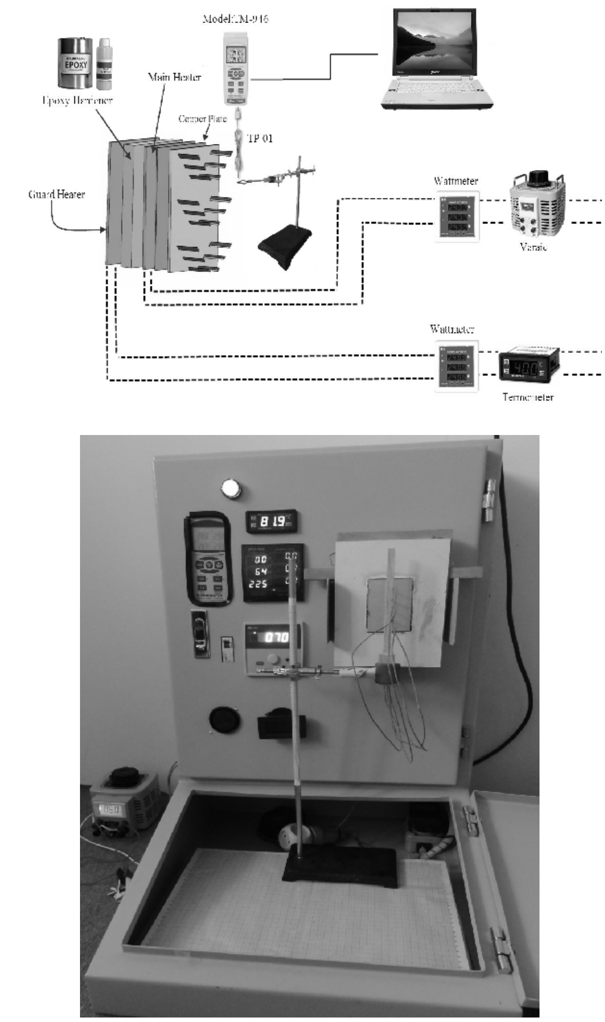

Fig. 3. Schematic view of experimental setup and experimental apparatus.

$$M = f(x_1, x_2, ..., x_N)$$

$$U(M) = \left\{ \sum_{i=1}^{N} \left[\frac{\partial f}{\partial x_i} U(x_i) \right]^2 \right\}^{\frac{1}{2}} \qquad (2)$$

where f is the function of M in terms of input, estimates x_1, x_2, . . ., x_N, and each $U(x_i)$ is a standard input uncertainty. Table 1 lists the experimental values of the directly measured parameters and the associated uncertainties. Thus, the experimental uncertainties of the convection heat transfer coefficient were estimated to be -3.5%.

3. Analysis and modeling

The basic geometry of fin configuration which is studied in this article, and is fabricated by CNC machine tool, is shown in Fig. 4. The numerical simulation was conducted using Fluent V6.3, a commercially available CFD code based on the finite volume method. The convergence of the computational solution is determined based on residuals for the continuity and energy equations.

Table 1. Measuring instruments range and accuracy.

Description	Model	Range	Accuracy
Temp. of ambient	K type	-200 to 1000	±0.1℃
Temp. of surtace	K type	-200 to 1000	±0.1℃
Voltage measurement	Variac	0 to 400	±0.1 V
Ampere-meter	Multimeter	0 to 20	±0.1 A
Lentgh measurement	Caliper	6	±0.001 m

Fig. 4. Fabricated geometry of V-type fin.

Solid modeling, computational grid generation and meshing were done using Gambit Preprocessor 2.2.30 Software. In Gambit session, the base plate, the fin configurations and heaters were defined as the walls, all other remaining boundaries were defined as pressure outlet.

The grid dependence was investigated by varying the number of grid points from 22,680 to 285,714. We selected 65,016 grid points. Governing equations are solved using a finite volume approach. The convective terms are discretized using the power-law scheme, whereas for diffusive terms the central difference is employed. Coupling between the velocity and pressure is made with SIMPLE algorithm. The resultant system of discretized linear algebraic equations is solved with an alternating direction implicit scheme.

The governing equations which is used, in this study are as follows.

Continuity equation:

$$\frac{\partial(\rho u)}{\partial x} + \frac{\partial(\rho v)}{\partial y} + \frac{\partial(\rho w)}{\partial z} = 0 . \qquad (3)$$

X-momentum equation:

$$\frac{\partial\left(\rho u^2\right)}{\partial x} + \frac{\partial\left(\rho uv\right)}{\partial y} + \frac{\partial\left(\rho uw\right)}{\partial z} = -\frac{\partial p}{\partial x} + \mu\left(\frac{\partial^2 u}{\partial x^2} + \frac{\partial^2 u}{\partial y^2} + \frac{\partial^2 u}{\partial z^2}\right) + \frac{\partial}{\partial y}\left(\mu\frac{\partial u}{\partial y}\right). \qquad (4)$$

Y-momentum equation:

$$\frac{\partial(\rho vu)}{\partial x}+\frac{\partial(\rho v^2)}{\partial y}+\frac{\partial(\rho vw)}{\partial z}= -\frac{\partial p}{\partial y}+\mu\left(\frac{\partial^2 v}{\partial x^2}+\frac{\partial^2 v}{\partial y^2}+\frac{\partial^2 v}{\partial z^2}\right)+g(\rho-\rho_\infty). \tag{5}$$

Z-momentum equation:

$$\frac{\partial(\rho wu)}{\partial x}+\frac{\partial(\rho wv)}{\partial y}+\frac{\partial(\rho w^2)}{\partial z}= -\frac{\partial p}{\partial z}+\mu\left(\frac{\partial^2 w}{\partial x^2}+\frac{\partial^2 w}{\partial y^2}+\frac{\partial^2 w}{\partial z^2}\right). \tag{6}$$

Energy equation:

$$\left(\frac{\partial(\rho uT)}{\partial x}+\frac{\partial(\rho vT)}{\partial y}+\frac{\partial(\rho wT)}{\partial y}\right)= \frac{K}{C_p}\left(\frac{\partial^2 T}{\partial x^2}+\frac{\partial^2 T}{\partial y^2}+\frac{\partial^2 T}{\partial z^2}\right). \tag{7}$$

For the numerical analysis, the following assumptions are applied.

(1) The flow is steady, laminar, and three-dimensional.

(2) Aside from density, the properties of the fluid are independent of temperature.

(3) Air density is calculated by treating air as an ideal gas.

(4) Radiation heat transfer is negligible.

The average convection heat transfer coefficient $\bar{h}$ is calculated by

$$\bar{h}=\frac{Q}{A_h(T_b-T_\infty)}. \tag{8}$$

The average Nusselt number $\overline{Nu}$ is calculated by

$$\bar{Nu}=\frac{\bar{h}L}{k_a} \tag{9}$$

where k_a is evaluated at the film temperature T_f $(T_f=\frac{T_b-T_\infty}{2})$.

4. Results and discussion

The numerical and experimental results are validated. In this study, to verify the numerical and experimental results, the results which are gained from this study for laminar air flow over a vertical plate with length 0.08 m were plotted with Churchill and Chu [6], Eq. (10), and McAdams [7], Eq. (11), correlations, as displayed in Fig. 5. These results reveal that except for the McAdams' correlation, which is a very rough correlation, the experimental and numerical results are to the same extent in good agreement with the results from literature.

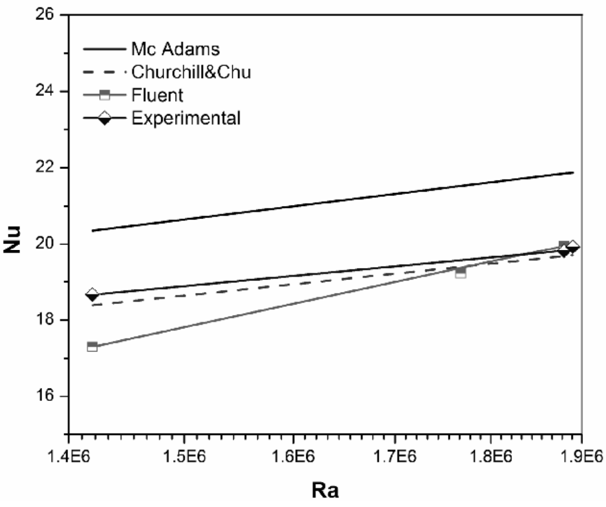

Fig. 5. Verifying the experimental and numerical results.

The average error between experimental and numerical results is 6.0%.

$$\mathrm{Nu}=0.68+\frac{0.67(\mathrm{Ra})^{\frac{1}{4}}}{\left(1+\left(\frac{0.492}{\mathrm{Pr}}\right)^{\frac{9}{16}}\right)^{\frac{4}{9}}} \tag{10}$$

$$\mathrm{Nu}=0.59\ (\mathrm{Ra})^{\frac{1}{4}} \qquad 10^4<\mathrm{Ra}<10^9. \tag{11}$$

Fig. 6 shows the schematic view of studied fin configurations. By studying these cases, the effect of the number, gap (d) and also the shape of pieces on natural convection heat transfer are studied.

As shown in Fig. 7, the heat transfer coefficients of cases 2-4 are smaller to that of case 1. The cause of this reverse pattern is that when the pieces are at the minimum space (cases 2-4), on the one hand, fin configuration (unlike case 1) lost its suction ability (The low pressure region created at the apex zone of V fin enabling suction effect). On the other hand, due to the small distance between the pieces of fins, there is no possibility of free flow of air around the pieces and fins act as barrier against air flow. Then, these three cases have smaller heat transfer coefficient than case 1. The increase in the number of pieces, cases 2-4, and gap between them, cases 4-6, leads into an increase in the ratio of natural convection heat transfer coefficient for fin configuration, regardless of base plate, to that of vertical plate. In addition, the effect of changes in the shape of small edges on the pieces is studied. In cases 6 and 7, these edges are both vertical and horizontal, respectively. In cases 8 and 9, one edge is vertical and the other is horizontal for each of them. According to this figure, with constant number of pieces and "d", the ratio of natural convection heat transfer coefficient for fin configuration, regardless of base plate, to that of vertical plate is maximized for case 8.

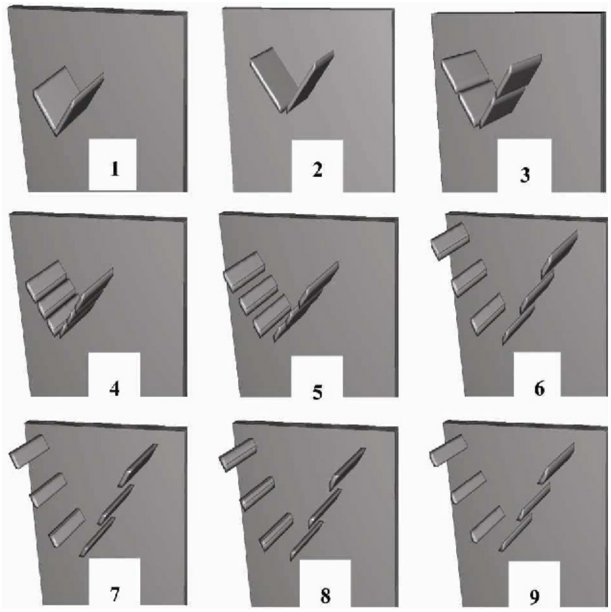

Fig. 6. Schematic view of studied fin configurations.

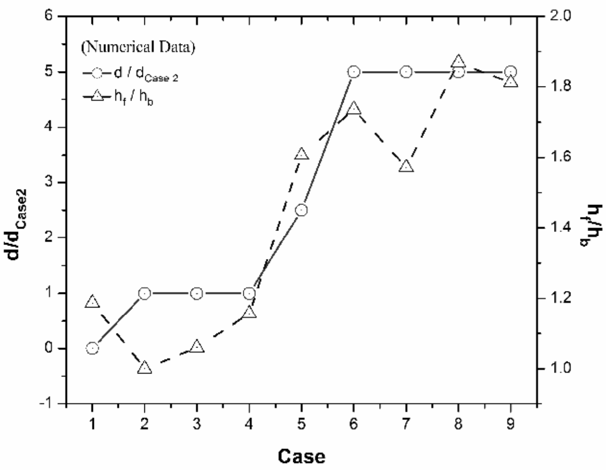

Fig. 7. The ratio of natural convection heat transfer coefficient for the 9 cases (Numerical data).

The effect of varying the space between the rows is also studied for the optimum fin shape in one row and on the vertical base. Table 2 denotes the dimensions and characteristics of different uniform fin configurations for aluminum heat sinks which are considered in the present work. Fig. 8 illustrates at a given difference between base and ambient temperature, the thermal resistance of fin array decreases with respect to the decrease in dimensionless parameter of row spacing, in other words by increasing the number of fins, thermal resistance decreases. The variation of heat transfer coefficient of fin configurations versus row spacing (S), at two different temperature difference, is shown in Fig. 9. At a given difference between base and ambient temperature, the natural convection heat transfer coefficient of fin array increases with respect to the increase in row spacing and reaches a maximum; then, it falls. The row spacing value, for which the natural convection heat transfer coefficient is maximum, is called optimum row spacing. In this case study, the optimum row spacing is 15 mm (Type-c).

Table 2. Dimensions of the fin configurations.

Fin-type	Fin height H(mm)	Row spacing S(mm)	Number of rows (n)	Fin thickness t(mm)
Type-a	15	80	1	1
Type-b	15	30	3	1
Type-c	15	15	5	1
Type-d	15	7.5	9	1
Type-e	15	6	11	1
Type-f	15	5	13	1
Type-g	15	4	16	1
Base length (L=80 mm)			Base width (W=59.8 mm)	

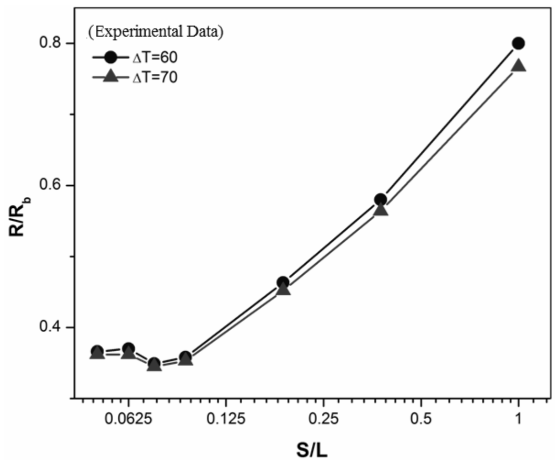

Fig. 8. Thermal resistance of fin configurations vs dimensionless parameter of row spacing (S\L) (Experimental date).

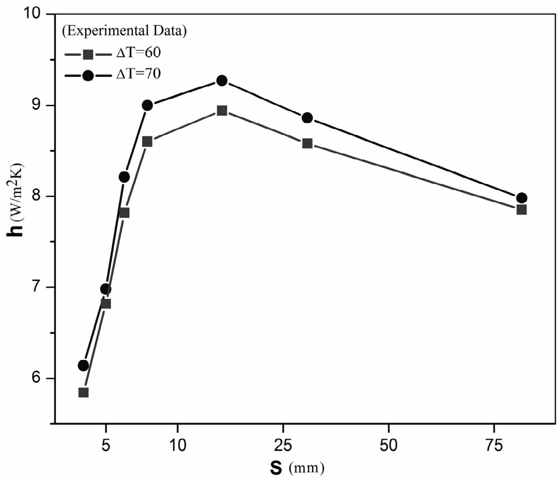

Fig. 9. Variation of heat transfer coefficient of fin configurations with S\L.

It is possible to reach to a useful correlation for laminar air which relates the Nusselt number to the Rayleigh number.

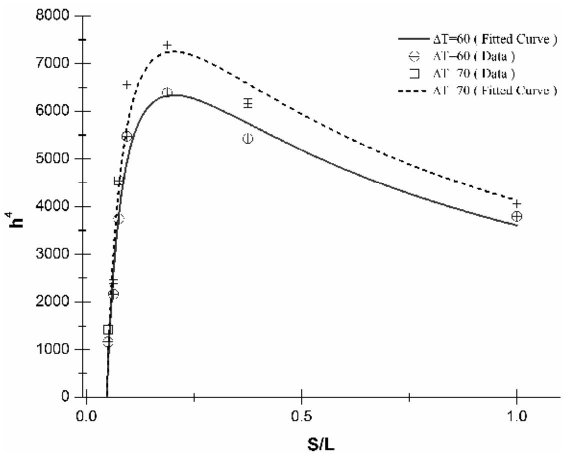

Fig. 10. Variation of the forth power of natural convection heat transfer coefficient with S\L.

According to the most of laminar natural convection correlations, the Nusselt number is proportional to $\mathrm{Ra}^{0.25}$. In this correlation, the Rayleigh number has the same power (0.25). Therefore, the variation of the forth power of natural convection heat transfer coefficient versus dimensionless parameter of row spacing (S\L) is plotted in Fig. 10. Rational curve fitting of this data (Nelder function, Eq. (12)) results in the determination of the correlation of forth power of natural convection heat transfer coefficient versus S\L, Eq. (13). Then, having defined the modified Rayleigh number as Eq. (14), and having substituted Eq. (14) into Eq. (13), a correlation for variation of Nusselt number versus modified Rayleigh number, as Eq. (15), is obtained.

$$y = \frac{(x+a)}{(b0 + b1*(x+a) + b2*(x+a)^2)} \tag{12}$$

$$h^4 = \left(\frac{k}{L}\right)^4 \frac{g\beta L^3 (T_S - T_\infty)}{\upsilon\alpha} \tag{13}$$

$$\frac{3.47\times10^{-5}\left(\dfrac{S}{L}-0.0463\right)}{4.36\times10^{-6}+1.02\times10^{-4}\left(\dfrac{S}{L}-0.0463\right)+1.79\times10^{-4}\left(\dfrac{S}{L}-0.0463\right)^2}$$

$$Ra_L' = \frac{g\beta L^3 (T_S - T_\infty)}{\upsilon\alpha} \tag{14}$$

$$\frac{3.47\times10^{-5}\left(\dfrac{S}{L}-0.0463\right)}{4.36\times10^{-6}+1.02\times10^{-4}\left(\dfrac{S}{L}-0.0463\right)+1.79\times10^{-4}\left(\dfrac{S}{L}-0.0463\right)^2}$$

$$Nu_L = 0.07675 Ra_L'^{\,0.25}. \tag{15}$$

To dig out the reason why by increasing the number of fins, more than optimum number, natural convection heat transfer decrease, the heat transfer coefficient and temperature distributions are investigated for type g. According to Fig. 11, for each row, the thermal boundary layer is formed in the vicinity

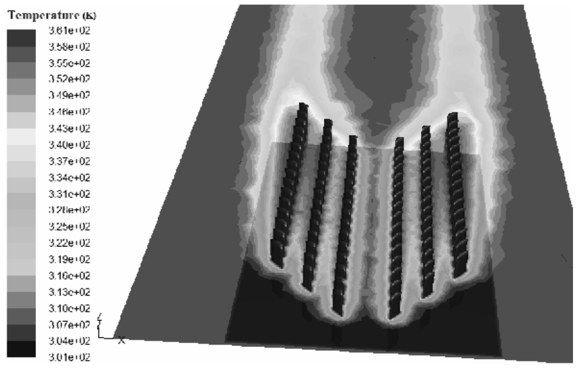

Fig. 11. Temperature distribution of the Type-g.

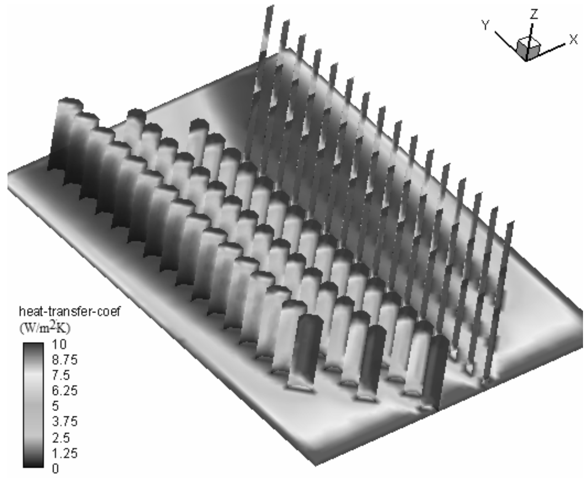

Fig. 12. Variation of heat transfer coefficient contour of the Type-g.

of lateral faces of the pieces and as it goes distant from pieces, this boundary layer vanishes. However, due to the boundary layers interferences, the boundary layers would slowly dissipate in the air flow which, in turn, would result in an extremely thick boundary layer. The thicker the boundary layer, the less the heat transfer coefficient will be (Fig. 12).

5. Conclusions

In this article, first, the shape and the number of pieces and the gap between the pieces in different cases of V-type fin configuration were studied in laminar natural convection condition, both experimentally and numerically. By increasing the number of pieces, and the gap between them, the ratio of natural convection heat transfer coefficient of fin configuration, without considering the effect of base plate, to natural convection heat transfer coefficient of vertical plate, increased. For different cases the natural convection heat transfer rate, the natural convection coefficient, the thermal boundary layer and the laminar flow of the air evaluated and optimum shape is selected. The results show that the maximum natural convection coefficient and also the maximum natural convection heat transfer rate, takes place for the case in which the fin has the least effect on the air flow in the vicinity of base plate and also the thickness of thermal boundary layer on the fin is fine. After finding the optimum shape, the row spacing is studied, with an increase in the number of rows (a decrease in row spacing) natural convection heat transfer coefficient increases primarily, reaches a maximum value where the optimum row spacing is defined and, then, due to the interference of boundary layers of rows, steeply decreases Finally, a correlation is also presented relating the Nusselt number with the modified Rayleigh number.

Nomenclature

A	: Area (m^2)
A_h	: Heating area (m^2)
c_p	: Coefficient of heat capacity ($J/(kg^\circ c)$)
d	: Gap between pieces (mm)
g	: Gravitational acceleration (m^2/s)
k	: Thermal conductivity ($W/m^\circ c$)
h	: Convection heat transfer coefficient (W/m^2K)
L	: Fin length (mm)
n	: Number of rows
Nu	: Nusselt number
P	: Pressure (N/m^2)
pr	: Prandtl number
q"	: Heat flux (W/m^2)
Ra	: Rayleigh number
S	: Row spacing (mm)
T	: Temperature (K or $^\circ c$)
U	: Total uncertainty
u,v, w	: Velocity in x, y, z directions respectively (m/s)
x, y, z	: Cartesian coordinate (m)

Greek symbols

α	: Thermal diffusivity (m^2/s)
β	: Coefficient of volumetric expansion (K^{-1})
μ	: Dynamic viscosity (N/m^2s)
ρ	: Density (kg/m^3)
v	: Kinematic viscosity (m^2/s)
ΔT	: Base to ambient temperature difference (K)

Subscripts

a	: Ambient
avg	: Average
b	: Base plate
exp	: Experimental
f	: Fluid(air)
∞	: Ambiant

References

[1] T. Misumi and K. Kitamura, Natural convection heat transfer from a vertical heated plate with a horizontal partition plates, *J.S.M.E. Int. J. Heat Mass Transfer*, 38 (1990) 463-470.

[2] R. L. Edlabadkar, N. K. Sane and G. V. Parishwad, Computational analysis of natural convection with single V-type partition plate, *Proc. 5th European Thermal-Sciences Conf.*, The Netherlands (2008).

[3] S. H. Bhavnani and A. E. Bergles, Effect of surface geometry and orientation on laminar natural convection heat transfer from a vertical flat plate with transvers roughness elements, *International Journal of Heat and Mass Transfer*, 33 (5) (1990) 965-981.

[4] N. Heya, M. Takeuchi and T. Fujii, Influence of various surface roughness's on free convection heat transfer from a horizontal cylinder, *Chemical Engineering Journal*, (23) (1982) 185-190.

[5] V. S. Arpaci, *Conduction heat transfer*, Addison-Wesley Publishing Company (1966).

[6] S. W. Churchill and H. H. S. Chu, Correlating equations for laminar and turbulent free convection from a vertical plate, *International Journal of Heat Mass Transfer*, (18) (1995) 1323-1329.

[7] W. H. McAdams, *Heat transmission*, 3rd ed., McGraw-Hill Book Co., NY (1954).

[8] R. J. Moffat, Describing the uncertainties in experimental results, *Experimental Thermal and Fluid Science*, (1) (1988) 3-17.

Mohammad Mahdi Naserian started to study M. Sc. in Mechanical Engineering at IAUM in 2008. His research is diversified in the areas of theoretical and numerical modeling of natural convection heat transfer and electronic cooling. He has more than 9 dissertations in National & International Conferences and also 3 International Journals. In 2011, he graduated as the top student. He is currently phd student at Sistan & Baluchestan University of Iran.

Mahdi Fahimina started to study M. Sc. in Mechanical Engineering at IAUM in 2008. His research is diversified in the areas of theoretical and numerical modeling of natural convection heat transfer and electronic cooling. He has more than 9 dissertations in National & International Conferences and also 3 International Journals.

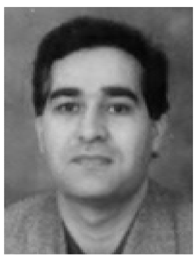

Hamid Reza Goshayeshi has an Hons. Degree in Chemical Engineering, M. Sc. and Ph. D. in Mechanical Engineering from South Bank University in London and did his post doctoral research on "Improvement of the Rankin Cycle". He served as Assistant Professor in Azad University (Iran) and presently is serving as Vice Chancellor for research in Mashad Azad University (Iran).